acta physica slovaca vol. 56 No. 3, 299 – 303 **June 2006**

PRODUCTION OF ω IN pd $\rightarrow$ ^{3}Heω AT KINEMATIC THRESHOLD[1]

K. Schönning for the CELSIUS/WASA collaboration[2]
Department of Radiation Sciences, Uppsala University, Box 535, S-75121, Uppsala, Sweden

Received 3 November 2005, in final form 10 January 2006, accepted 3 February 2006

Production of ω in the pd $\rightarrow$ ^{3}Heω reaction is currently being studied at the CELSIUS storage ring with the WASA 4π detector. Older data on ω production from various experiments show a suppression in the cross section near the kinematic threshold. New data have been collected with WASA during 35 eight-hour shifts. A preliminary analysis of these data shows ω production in the pd $\rightarrow$ ^{3}Heω reaction.

PACS: 25.40.Ve, 25.10.+s,

1 Introduction

Forward and backward ω production in the π^-p $\rightarrow$ nω reaction was studied for final state CM (centre of mass) momenta up to $p^*_\omega = 260$ MeV/c by Binnie *et al.* [1] in the early seventies. It was found that the cross section was unexpectedly suppressed near threshold. The results were later confirmed by the same group using an extended experimental setup allowing smaller p^*_ω [2] and even later with a setup covering the full ω angular distribution [3]. It was first suggested that the drop in the cross section near threshold could be an effect of one of the pions from the ω decay being rescattered by the neutron. However, this effect should be stronger in the $\omega \rightarrow \pi^+\pi^-\pi^0$ decay channel (BR=89.1%) than in the $\omega \rightarrow \pi^0\gamma$ decay channel (BR=8.7%). Both channels were studied in [1, 2] and no difference in the momentum dependence of the cross section was observed for the two decay channels. A combination of S-wave and P-wave resonances was instead believed to give the strong momentum dependence observed near threshold.

In the mid-nineties, Wurzinger *et al.* studied ω production in pd $\rightarrow$ ^{3}Heω at SATURNE at 20 different beam energies [4]. This experiment did not separate the decay channels. The differential cross section for ω production at $\theta^*_\omega = 180^\circ$ turned out to be suppressed for $p^*_\omega \leq 180$ MeV/c in a way similar to the threshold suppression of π^-p $\rightarrow$ nω.

However, in [5, 6] it is discussed whether the interpretation of the data given in [1–4] is incorrect and in [6] the need of more data is stressed.

The CELSIUS/WASA collaboration hopes to bring some clarity into the issue by adding new data to the existing sample. Data have been taken at two different beam energies, 24 eight-hour shifts at $T_p = 1450$ MeV and 11 shifts at $T_p = 1360$ MeV, which correspond to $p^*_\omega = 280$ MeV/c

[1] Presented at the Workshop on Production and Decay of η and η' Mesons (ETA05), Cracow, 15–18 September 2005.
[2] E-mail address: karin.schonning@tsl.uu.se

and $p^*_\omega = 144$ MeV/c , respectively. Thus we will obtain one cross section measurement well above the threshold region and one within the energy range where the suppression in the differential cross section has been observed. We will measure all final state particles and thereby separate the two most important decay channels. In addition, we will measure the angular distributions of the ω meson and its decay products. In Section 2, the WASA detector, the ^{3}He triggers and the method used for offline identification of ^{3}He will be presented. In section 3, the current status of the analysis will be given. Finally we will summarise and discuss future prospects.

2 The CELSIUS/WASA experiment

Our measurements have been performed at the The Svedberg Laboratory in Uppsala, Sweden. The WASA (Wide Angle Shower Apparatus) detector [7] was, until June 2005, an integrated part of the CELSIUS (Cooling with ELectrons and Storing of Ions from Uppsala Synchrocyclotron) storage ring. A proton beam and a deuterium pellet target [8] was used. The ^{3}He was detected in the forward detector, covering a polar angle range from 3° to 18°, which corresponds to 95% of the ^{3}He phase space in pd $\rightarrow$ ^{3}Heω at $T_p = 1450$ MeV and 78% at $T_p = 1360$ MeV. The forward detector consists of a sector-like window counter (FWC) for triggering, a proportional chamber for precise angular information, a trigger hodoscope (FTH) for triggering and offline particle identification, a range hodoscope (FRH) for energy measurements and particle identification and a veto hodoscope for triggering.

The charged pions from the ω decay can be detected in the forward detector as well as in the central detector. In the central detector, their momenta are estimated by tracking in a magnetic field using the mini drift chamber. The plastic scintillation barrel, used for particle identification and for angular information, covers an angular range from 24° to 159°. The central scintillator calorimeter measures angles and energies of photons from meson decays.

The ^{3}He trigger is based on the fact that ^{3}He, due to its higher charge, deposits more energy in a given detector layer than protons and deuterons with the same velocity. The FWC consists of twelve sectors of scintillating material, each one equipped with a photomultiplier. Requiring a large energy deposit in the FWC would thus select events with ^{3}He in the final state and reject most protons and deuterons. Figure 1 shows Monte Carlo simulations of the energy deposit in the FWC for particles coming from reactions with ^{3}He in the final state (pd $\rightarrow$ ^{3}Heω and pd $\rightarrow$ ^{3}He$2\pi^0$) and without ^{3}He (pd $\rightarrow$ pd and quasi-free pd $\rightarrow$ ppn). It is indeed clear that the energy deposit peaks for the two types of reactions are well separated. However, looking closer it turns out that the high energy deposit tails of protons and deuterons overlap with the energy deposit peak of the ^{3}He. The areas under the curves are arbitrary and are thus not normalised to the cross sections of the four reactions. In fact, at this energy, the cross section of pd $\rightarrow$ pd [9] and quasi-free pd $\rightarrow$ ppn [10] are expected to be $10^4 - 10^6$ times larger than the pd $\rightarrow$ ^{3}Heω [4] which means that the high energy deposit tails of the two former reactions are important, as we shall see.

In order to reject particles not coming from the target interaction point, an additional requirement was applied: matching in the azimuthal angle ϕ between the hit in the FWC and the hit in one of the sector-like detector layers downstream of the FWC, either the third layer of the FTH or the first layer of the FRH. A trigger requiring high energy deposit in the FWC and a matching hit in the FTH or the FRH has typically a relative ^{3}He yield of 1%. Around 50% of the events

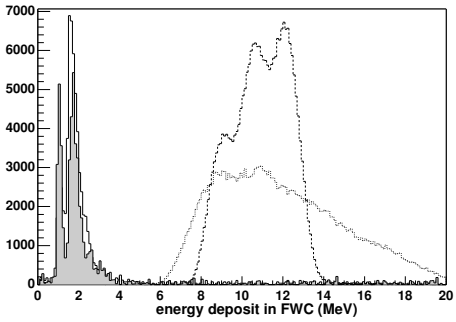

Fig. 1. Monte Carlo simulations of the energy deposit in the FWC for different reactions at $T_p = 1450$ MeV. The filled histogram comes from quasi-free pd $\rightarrow$ ppn, the solid line histogram from pd $\rightarrow$ pd, the thin dashed line from pd $\rightarrow {}^3$Heω and the dotted line from pd $\rightarrow {}^3$He$2\pi^0$.

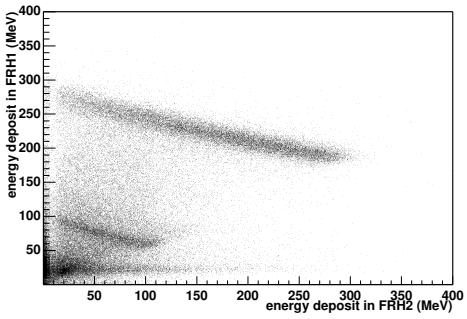

Fig. 2. The energy deposit in the first layer of the FRH *versus* the energy deposit in the second layer of the FRH, for particles stopping in the second layer of the FRH. The clear uppermost band corresponds to ^{3}He, below the proton and the pion bands are seen. The data are from December, 2004.

accepted by the trigger contain slow protons, a consequence of the high energy deposit tails. The data aquisition system used [11] was fast enough to allow for a high aquisition rate (2-3 kHz, with life time $\approx 70\%$). Furthermore, the trigger selects all channels with ^3He in the final state, which allows for cross section measurements of a large number of reactions.

The particles in the Forward Detector are identified by comparing the energy deposit in the layer where they stop to the energy deposit in the preceding layer. Different particles will then show up in different bands, as illustrated in figure 2, where the ^{3}He are seen clearly in the uppermost band. Below, a clear band corresponding to protons appears and further below a band with fast pions.

3 Results from analysis of December 2004 data

The data presented here were taken in December 2004, during four eight-hour shifts. The experiment was running in a test mode, which means the triggers were not yet fully tested and optimised. Besides, an older data aquisition system was used that was considerably slower than the system taken into operation in March 2005. It was therefore necessary, in addition to the trigger condition mentioned in section 2, to introduce vetos on more than one hit in the FTH and on hits in the veto hodoscope in order to reduce the trigger rate. The conditions were thus not optimal for the $\omega \rightarrow \pi^+\pi^-\pi^0$ channel, since some good events had to be rejected by the trigger when one of the charged pions was emitted in the direction of the forward detector. In later run

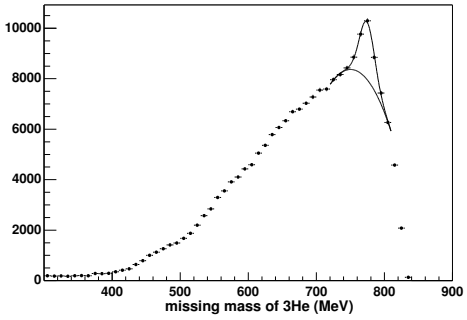

Fig. 3. The missing mass distribution of the ^{3}He, for all ^{3}He candidates in the December 2004 data. The lines show the fitted gaussian peak on top of a polynomial background and the fitted polynomial, respectively.

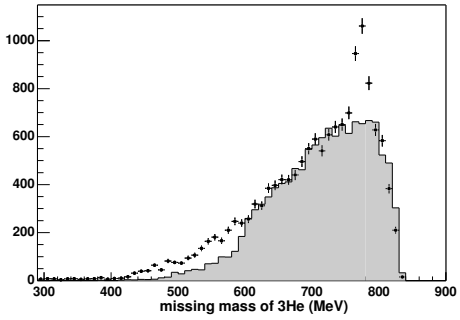

Fig. 4. The dots show the missing mass distribution of ^{3}He for events with one ^{3}He, two photons and two charged tracks identified from December 2004 data. The filled histrogram shows the ^{3}He missing mass distribution for pd $\rightarrow$ ^{3}He + $\pi^+\pi^-\pi^0$ obtained from Monte Carlo simulations.

periods, the faster data aquisition system allowed for less selective triggers and the vetos were abandoned.

At the beam energy $T_p = 1450$ MeV, 175000 ^{3}He candidates were indentified, whose missing mass distribution is shown in figure 3. The acceptance for pd $\rightarrow$ ^{3}Heω, $\omega \rightarrow \pi^+\pi^-\pi^0$ is 36% and for pd $\rightarrow$ ^{3}Heω, $\omega \rightarrow \pi^0\gamma$ it is 40%. The difference in acceptance is a consequence of the vetos in the trigger. By fitting a gaussian peak on a polynomial background and subtracting the background, the number of ω candidates was estimated to 6300. The position and the width of the ω peak is consistent with Monte Carlo simulations.

To identify the $\omega \rightarrow \pi^+\pi^-\pi^0$ decay channel, events with one ^{3}He, two additional charged tracks and two photons (from the π^0 decay) were selected. According to Monte Carlo simulations, the acceptance with these constraints is 6%. The missing mass distribution of ^{3}He is shown in figure 4. From fitting a gaussian peak on top of a polynomial background, 1100 $\omega \rightarrow \pi^+\pi^-\pi^0$ candidates were identified. This is roughly consistent with what we expect, having 6300 candidates without constraints and taking the BR and acceptances into account. The effects of the applied constraints are thus well understood. The main source of uncertainty is likely to be systematic uncertainties in the curve fitting procedure.

The most important background channel is prompt 3π production in pd $\rightarrow$ ^{3}He$\pi^+\pi^-\pi^0$, since it has the same signature as pd $\rightarrow$ ^{3}Heω, $\omega \rightarrow \pi^+\pi^-\pi^0$. The acceptance of prompt 3π production is 5%. The simulated ^{3}He missing mass for the former channel is shown in the filled histogram in figure 4. The normalisation is chosen to fit the data, and the background is indeed well described by the pd $\rightarrow$ ^{3}He$\pi^+\pi^-\pi^0$ channel between 600 MeV and 850 MeV. At lower

energies, we expect a small contribution from pd $\rightarrow$ ^{3}Heη, $\eta \rightarrow \pi^+\pi^-\pi^0$. This cross section has been measured at SATURNE at $T_p = 1450$ MeV to $\approx 200\ nb$ [12]. The acceptance in WASA with the given constraints is 2.4% and the BR of the $\eta \rightarrow \pi^+\pi^-\pi^0$ decay mode is 23%. The total cross section of pd $\rightarrow$ ^{3}Heω should be roughly $200\ nb$, from extrapolating the result in [4]. The η peak is thus expected to be around ten $((0.06 * 0.891)/(0.024 * 0.23))$ times smaller than the ω peak in Figure 4. Furthermore the peak is expected to be broader, as a consequence of kinematics: a ^{3}He from pd $\rightarrow$ ^{3}Heη at a given beam energy has higher kinetic energy than a ^{3}He from pd $\rightarrow$ ^{3}Heω and will thus traverse more detector material before it is stopped. The energy resolution of a particle becomes worse the more detector material it traverses. These are the main reasons why no clear η peak appears in figure 4. However, the small enhancement in the data between 500 MeV and 600 MeV, compared to the simulations of prompt 3π production, might be due to η production.

4 Summary and outlook

Studying the ω production is well motivated, since old data at threshold are not fully understood and only little data cover a larger part of phase space. The CELSIUS/WASA collaboration has been collecting data at two different beam energies and for two different decay channels. The WASA setup covers a large part of the phase space of the ω as well as its decay products. The triggers select all reactions with ^{3}He in the final state, which makes it possible to study not only the ω production but also the background channels, such as multi-pion production, η production and $\eta\pi^0$ production. The four shifts of data analysed so far show promising results: ω candidates are indeed seen and the position and width of the ω peak is consistent with Monte Carlo simulations. There are 31 more shifts of data to be analysed. This means that a lot of hard work remains. Hopefully, interesting results will emerge.

Acknowledgement: Financial support is acknowledged from the Swedish Research Council and the European Community Research Infrastructure Activity under FP5 'Structuring the European Research Area' program (Hadron Physics, contract number R113-CT-2004-506078)

References

[1] D.M. Binnie *et al.*: *Phys. Rev. D* **8** (1973) 2789
[2] J. Keyne *et al.*: *Phys. Rev. D* **14** (1976) 28
[3] H. Karami *et al.*: *Nucl. Phys. B* **154** (1979) 503
[4] R. Wurzinger *et al.*: *Phys. Rev. C* **51** (1995) R443
[5] C. Hanhart, A. Kudryavtsev: *Eur. Phys. J. A* **6** (1999) 325-328
[6] C. Hanhart, A. Sibirtsev, J. Speth: *FZJ-IKP-TH-2001, hep-ph/0107245*
[7] J. Zabierowski *et al.*: *Physica Scripta T* **99** (2002) 159-169
[8] C. Ekström *et al.*: *Physica Scripta T* **99** (2002) 169-173
[9] H. Rohdjess *et al.* : *Phys. Rev. C* **57** (1998) 2111
[10] V.M. Baturin *et al.* : *Yad. Fiz.* **31** (1980) 397-402
[11] J. Zlomanczuk: $http://www4.tsl.uu.se/\tilde{}jozef/wasa4pi/DAQ/newdaq.html$
[12] T. Kirchner: *Ph.D. thesis, Institute de Physique Nucleaire*, Orsay 1993